Hindawi
Cellular Microbiology
Volume 2022, Article ID 5431666, 14 pages
https://doi.org/10.1155/2022/5431666

Research Article

A Model of Intracellular Persistence of *Pseudomonas aeruginosa* in Airway Epithelial Cells

Julien K. Malet,[1] **Lisa C. Hennemann**,[1,2] **Elizabeth M.-L. Hua**,[2] **Emmanuel Faure**,[3,4] **Valerie Waters**,[5] **Simon Rousseau**,[1] **and Dao Nguyen**[1,2,6]

[1]*Meakins Christie Laboratories, Research Institute of the McGill University Health Centre, Montreal, Quebec, Canada*
[2]*Department of Microbiology and Immunology, McGill University, Montreal, Quebec, Canada*
[3]*Univ. Lille, U1019-UMR 9017-CIIL-Center for Infection and Immunity of Lille, F-59000 Lille, France*
[4]*CHU Lille, Service Universitaire de Maladies Infectieuses, F-59000 Lille, France*
[5]*Division of Infectious Diseases, Department of Pediatrics, The Hospital for Sick Children, University of Toronto, Toronto, CA, Canada*
[6]*Department of Medicine, McGill University, Montreal, Quebec, Canada*

Correspondence should be addressed to Dao Nguyen; dao.nguyen@mcgill.ca

Julien K. Malet and Lisa C. Hennemann contributed equally to this work.

Received 30 January 2022; Accepted 1 July 2022; Published 12 August 2022

Academic Editor: Barbara Kahl

Pseudomonas aeruginosa (*P.a.*) is a major human pathogen capable of causing chronic infections in hosts with weakened barrier functions and host defenses, most notably airway infections commonly observed in individuals with the genetic disorder cystic fibrosis (CF). While mainly described as an extracellular pathogen, previous *in vitro* studies have described the molecular events leading to *P.a.* internalization in diverse epithelial cell types. However, the long-term fate of intracellular *P.a.* remains largely unknown. Here, we developed a model allowing for a better understanding of long-term (up to 120 h) intracellular bacterial survival in the airway epithelial cell line BEAS-2B. Using a tobramycin protection assay, we characterized the internalization, long-term intracellular survival, and cytotoxicity of the lab strain PAO1, as well as clinical CF isolates, and conducted analyses at the single-cell level using confocal microscopy and flow cytometry techniques. We observed that infection at low multiplicity of infection allows for intracellular survival up to 120 h post-infection without causing significant host cytotoxicity. Finally, infection with clinical isolates revealed significant strain-to-strain heterogeneity in intracellular survival, including a high persistence phenotype associated with bacterial replication within host cells. Future studies using this model will further elucidate the host and bacterial mechanisms that promote *P. aeruginosa* intracellular persistence in airway epithelial cells, a potentially unrecognized bacterial reservoir during chronic infections.

1. Introduction

Many bacteria can survive within the intracellular host environment where they escape immune recognition, clearance by extracellular host defenses, and many antibiotics. While the intracellular lifestyle of obligate intracellular pathogens (e.g., *Chlamydia* and *Rickettsia* species) and facultative intracellular pathogens (e.g., *Listeria monocytogenes* and *Salmonella enterica*) has been extensively studied, the capacity for intracellular residence of other bacteria classically known as extracellular pathogens is less well appreciated. Several bacterial pathogens, such as *Staphylococcus aureus* and *Escherichia coli*, can invade, survive, and in some cases replicate within host cells. By adopting an intracellular lifestyle, their evasion of host defenses and antimicrobial therapy likely contributes to their ability to cause infections that persist or recur after antibiotic treatment [1, 2]. For example, uropathogenic *Escherichia coli* can persist within bladder epithelial cells for several weeks in murine models of urinary tract infections [3, 4], and its intracellular form has been

detected in urinary samples of patients with recurrent urinary tract infections [5, 6]. *Staphylococcus aureus* can invade different cell types, including phagocytes, epithelial, and endothelial cells *in vitro* [7–9], and its intracellular residence in nonphagocytic cells has been linked to chronic rhinosinusitis, osteomyelitis, and mastitis [10–13]. Not only are intracellular bacteria able to survive during antibiotic treatment, as many antibiotics show limited penetration and/or activity inside host cells, but intracellular bacteria may also serve as a reservoir for reinfection of surrounding tissue, thus contributing to the establishment of difficult to eradicate chronic infections [11, 14, 15].

Pseudomonas aeruginosa (*P.a.*) is an opportunistic gram-negative bacterium, primarily known as an extracellular pathogen capable of causing a wide spectrum of human infections. Notably, *P.a.* colonizes mucosal and external epithelial surfaces in hosts with impaired barrier functions and host defenses, causing chronic or subacute infections of different organs and tissues such as the cornea, soft tissue wounds, and airways [16]. Chronic *P.a.* airway infections are common in individuals with cystic fibrosis (CF) who carry mutations in the cystic fibrosis transmembrane conductance regulator (CFTR) gene, and in whom defects in mucociliary clearance and mucosal host immunity lead to impaired bacterial clearance [17]. Within respiratory secretions found in the airway lumen [18–21], *P.a.* can form biofilm microcolonies refractory to antibacterial killing and immune clearance [22, 23]. *P.a.* also subverts host immunity through a wide range of mechanisms [24], such as bacterial type 3 secretion system (T3SS)-mediated host cell killing [25], proteolytic degradation of proinflammatory and immune mediators [26–28], and exopolysaccharide overproduction [29]. While these host and antimicrobial evasion mechanisms have been extensively studied, the intracellular lifestyle of *P.a.* within airway epithelial cells and its potential contribution to the persistence of *P.a.* infections have been largely overlooked.

Previous *in vitro* studies have demonstrated *P.a.*'s ability to invade different epithelial and endothelial cell types. *P.a.* binds to the epithelium through interactions of bacterial adhesins (e.g., flagellum, type IV pilus, and LecA) [30–33] or other surface molecules (e.g., outer membrane porins and lipopolysaccharides) [34, 35] with host cell surface binding motifs (glycosphingolipid Gb3, N-glycosylated receptors, or heparan sulfate proteoglycans) [31, 32]. *P.a.'s* entry is an actin-dependent process which requires Rho family GTPases (Rho, Cdc42, or Rak1) for cytoskeletal remodeling [36, 37]. Recruitment of the host cell endocytic machinery is mediated by several signal transduction pathways, notably the phosphatidylinositol 3-kinase (PI3K)/PIP3/Akt pathway [30, 31, 38, 39], but also through activation of different tyrosine kinases, such as Src, Abl, and Fyn [37, 40, 41]. Studies examining the fate of intracellular *P.a.* [42–46] have primarily focused on short-term survival (typically 3 h to 8 h post-infection (p.i.)) and were performed in different epithelial cell types. Intracellular *P.a.* was described by the Fleiszig group to reside in nonapoptotic blebs, namely large cytosolic compartments generated by the detachment of host membranes from the cytoskeletal cortex [42, 43, 45, 47, 48]. Others observed intracellular *P.a.* in cytosolic dense aggregates called pod-like compartments similar to those formed by *E. coli* in bladder cells [44, 49] or in membrane-bound intracellular vesicles [39, 50].

Remarkably, the long-term fate of intracellular *P.a.* within epithelial cells is largely unknown. Garcia-Medina et al. assessed the long-term intracellular survival of the lab strain PAO1 in mouse tracheal epithelial cells and reported *P.a.* persistence without loss of host cell viability up to 72 h p.i [44]. More recently, Penaranda et al. assessed the intracellular survival of *P.a.* in the human 5637 bladder cell line and also observed bacterial survival up to 48 h p.i. without significant host cell death despite upregulation of the NF-κB signaling pathway [50]. Interestingly, results from several studies also suggest that the intracellular survival of *P.a.* clinical isolates may differ from laboratory strains such as PAO1 [50–53].

In order to better understand the intracellular persistence of *P.a.*, we developed a model of *P.a.* infection in airway epithelial cells that allowed the study of long-term (up to 120 h) intracellular bacterial survival. We characterized the infection kinetics with measurements of intracellular bacterial burden by viable bacterial counts and host cell cytotoxicity. For studies at the single-cell level, we validated analyses by flow cytometry, cell sorting, and confocal microscopy. Using this model, we also assessed several *P.a.* clinical isolates and demonstrated significant heterogeneity in the intracellular survival phenotype, including a high persistence phenotype.

2. Material and Methods

2.1. Bacterial Strains and Growth Conditions. Bacterial strains used in this study are listed in Supplementary Table S1. Bacterial strains were streaked from frozen stocks onto LB agar (BD Difco) (Wisent, 800-015) or LB agar containing 250 μg/mL carbenicillin (for PAO1-mCherry) and incubated overnight at 37°C. Isolated colonies were then inoculated in 5 mL of liquid LB media or LB media containing 250 μg/mL carbenicillin and incubated overnight at 37°C with shaking at 250 r.p.m. After 2 washes with sterile PBS (#311-010, Wisent), the bacterial cell pellets were resuspended in 5 mL of PBS to an optical density $OD_{600} = 0.9$, equivalent to ~10^9 CFU/mL. The initial dilution in PBS was followed by serial dilution in Dulbecco's modified Eagle's medium (DMEM, #319-005-CL, Wisent) supplemented with 10% heat-inactivated fetal bovine serum (FBS, #080-150, Wisent) to reach the desired multiplicity of infection (MOI).

2.2. Airway Epithelial Cell Culture Conditions and P.a. Infection. Immortalized human bronchial epithelial cells (BEAS-2B) were grown in DMEM supplemented with 10% heat-inactivated FBS and 50 IU/50 μg/mL penicillin/streptomycin (#450-200, Wisent) at 37°C with 5% CO_2. Once ~90% confluent, BEAS-2B cells were harvested and seeded at a density of 200,000 cells/mL (100,000 cells/well) in DMEM supplemented with 10% FBS in 24-well tissue culture plates

(#83.3922, Sarstedt) in the absence of antibiotics. After seeding, plates were incubated for 24 hours at 37°C prior to infection. The medium was then replaced by 500 μL of bacterial suspension at the required MOI in DMEM supplemented with 10% FBS (no antibiotics) and mixed by gentle shaking in a cross-wise manner. Plates were then centrifuged at 700 r.p.m. for 3 min to allow for bacterial adherence. After 4-h incubation at 37°C with 5% CO_2 for the internalization phase, tobramycin (#32986-56-4, Sigma-Aldrich) was added to each well to a final concentration of 100 μg/mL for 15 min (or until the end of infection when using clinical isolates) before harvesting for the $T = 4$–h time point. For later time points, the media was replaced by fresh DMEM (with 10% FBS) containing variable concentrations of tobramycin (25 μg/mL unless specified otherwise) for maintenance until cell harvest. For cell harvest, culture supernatants were first collected. Cells were then washed with PBS and lysed with 0.5% Triton X-100 (#9002-93-1, Sigma-Aldrich) in sterile PBS. Lysed cells were serially diluted in sterile PBS and plated on LB agar plates for bacterial growth. After overnight incubation at 37°C, CFU were counted to determine the viable intracellular bacterial load. Culture supernatants were also plated on LB agar plates to confirm the absence of extracellular bacteria in the cell culture media.

2.3. Cytotoxicity Assay. Epithelial cell viability was assessed using the lactate dehydrogenase (LDH) release/cytotoxicity assay, with measurement of LDH released by damaged cells into the culture supernatant and LDH in cell lysates as a measure of intact cell biomass (LDH assay kit, #11644793001, Sigma-Aldrich) according to the manufacturer's instructions. LDH concentrations were measured by absorbance at 492 nm (with reference wavelength subtraction at 690 nm), and cytotoxicity was expressed as the ratio of released LDH (in the supernatant) to total LDH (in the supernatant + cell lysate). To estimate the AEC biomass, we established a LDH standard curve using 10-fold dilution of BEAS-2B cells (from 1,000,000 cells to 5,000 cells) spun down, lysed with 0.5% Triton X-100 and used for LDH determination.

2.4. Flow Cytometry Analyses. Confluent BEAS-2B cells were harvested, seeded at a density of 200,000 cells/mL (200,000 cells/well) in DMEM supplemented with 10% FBS in 12-well tissue culture plates (#83.3921, Sarstedt), and infected with *P.a.* as described above. At the indicated time points following infection, culture supernatants were first collected to recover cells that had detached during the infection. Adherent cells were gently washed with PBS and incubated for 3 min at RT in PBS containing 1 mM EDTA (#60-00-4, Sigma-Aldrich) and 1 mM EGTA (#E4378, Sigma) to detach cells before harvesting by gentle pipetting. Cell suspensions were then pooled with their respective supernatants, centrifuged (2000 r.p.m for 5 min), and transferred to 96-well round-bottom plates (#82.1582, Sarstedt). Cells were then stained with 1 : 1000 Fixable Viability Dye eFluor 780 (FVD eF780, #65-0865-14, eBioscience) in PBS for 30 min on ice, followed by a wash with FACS buffer (PBS+0.5% FBS) and fixation in 0.5% PFA (#554655, BD Biosciences) for 10 minutes at RT. For cell sorting experiments, cells remained unfixed. Cells were then resuspended in FACS buffer for downstream analyses.

Stained cells were analyzed with an LSR II flow cytometer (BD Biosciences) and results were analyzed using FlowJo (BD Biosciences). Debris (low FSC-A, low SSC-A), doublets (SSC-A > SSC-H), and dead cells (high FVD eF780) were excluded. The gating for mCherry-positive cells was then defined for each experiment by exclusion of BEAS-2B cells infected with the nonfluorescent isogenic PAO1 strain (negative control) and restricting the false-positive mCherry signal to <0.5%. The proportion of dead cells was estimated as the percentage of dead cells among all single cells (after excluding debris and doublets).

2.5. Fluorescence-Activated Cell Sorting. For cell sorting, stained cells were resuspended at 5,000,000 cells/mL of FACS buffer before sorting using a BD FACSAria Fusion Cell Sorter (BD Biosciences). In order to validate the viability, plasmid expression, and amount of intracellular bacteria in mCherry-neg, mCherry-low, and mCherry-high populations, 10 and 100 cells for each population were sorted in 100 μL of lysis buffer (0.5% Triton X-100 in PBS) in a 96-well plate format at room temperature and processed for cell sorting validation.

To measure viable intracellular bacteria, sorted cells were lysed in 100 μL 0.5% Triton X-100 in PBS through vigorous pipetting. 45 μL of lysate were then plated on one regular LB agar plate and one LB agar plate containing 250 μg/mL carbenicillin, each. Plates were incubated overnight at 37°C, and CFU counts were enumerated the next day.

2.6. Detection of Intracellular P.a. by Immunofluorescence. BEAS-2B cells were seeded on uncoated sterile 15 mm or 12 mm round microscopy-grade borosilicate glass coverslips (0.13 to 0.17 mm thick, #12-545-80P or #22-031-145P, Fisherbrand) placed in 24-well plates and infected as described above (100.000 cells/well). At defined time points, cells were gently washed with PBS before fixation in 1% PFA for 15 min. Cells were then washed twice in PBS and blocked for 20 min at RT in staining solution (PBS+1% Bovine Serum Albumin (#A7906, Sigma-Aldrich) +1% goat serum (#G9023, Sigma-Aldrich)). Extracellular *P.a.* was first stained with a polyclonal anti-*P.a.* rabbit antibody (1 : 1000 dilution in staining solution, Abcam ab68538) for 45 min and counterstained for 30 min with an Alexa Fluor 647-conjugated antirabbit secondary goat antibody (1: 500 dilution, #A21-244, Life Technologies). Cells were then permeabilized with 0.2% Triton X-100 for 10 min, blocked, stained for both intracellular and extracellular *P.a.* (total *P.a.* stain) with the same polyclonal anti-*P.a.* rabbit antibody (1: 1000 dilution, Abcam ab68538) for 45 min, and counterstained for 30 min with an Alexa Fluor 488-conjugated antirabbit secondary goat antibody (1 : 500 dilution, #A11-008, Life Technologies) as well as DAPI nuclear stain (#LSD1306, Invitrogen) and TRITC-conjugated phalloidin (#5783, R&D) to stain the actin cytoskeleton. Samples were then mounted on glass coverslips using Fluoromount-G (#50-187-88, Thermo Fisher Scientific). Extracellular

*P.a.*was thus double stained by the extracellular and the total *P.a.* stains, while intracellular *P.a.*was single stained by the total *P.a.* stain.

2.7. Confocal Microscopy and Image Analysis. Samples were imaged with a Zeiss LSM700 confocal microscope equipped with 405 nm, 488 nm, 543 nm, and 633 nm lasers for the DAPI, AF488, TRITC, and AF647 channels, respectively. For each coverslip, 16 to 100 fields of view were randomly acquired (based on DAPI staining for focusing) with a 40× or 63× oil immersion objective for imaging of a minimum of 1000 (up to 9000) epithelial cells from at least 2 independent experiments. Z-stacks covering approximately 10-μm depth of the sample were acquired for maximum intensity Z-projection images. For each individual experiment, acquisition (including laser power, electronic gain, and background) and processing (fluorescence threshold) parameters were optimized for detection of host cells and bacteria using infected AEC and extracellular bacteria controls and kept constant for acquisition of all images. Intracellular bacteria were defined as a single green (Alexa Fluor 488) fluorescent signal at least 4 pixels in size (equivalent to approximately 500 nm) on maximum intensity Z-projection, located within the limits of the actin cytoskeleton (phalloidin staining). If any signal bigger than 2 pixels was also observed in the red channel (Alexa Fluor 647), the bacteria was considered as double positive and thus extracellular. For each image, the percentage of AEC harboring intracellular bacteria as well as the number of intracellular bacteria per AEC were reported. All images were randomly and manually analyzed by 2 blinded readers using ImageJ [54] software. Maximum intensity Z-projection images used for analysis are available at https://omero.med.ualberta.ca/webclient/?show=dataset-1152.

Automated analyses of confocal images (maximum intensity Z-projection) were also performed using a customized pipeline in Icy software [55] for counting of intracellular bacteria in eukaryotic cells (Icy analysis pipeline and script available as Supplementary methods and at https://omero.med.ualberta.ca/webclient/?show=dataset-1152). Eukaryotic cell segmentation was performed by active contouring of the cell nuclei using the actin signal as boundary. Identification of intracellular bacteria was based on spot detection (scale 2 parameter ≅3 pixel-sized objects) analysis performed on both red (extracellular stain) and green (total stain) channels, followed by colocalization analysis of the detected spots. Spots detected in the green channel that were not colocalized with spots in the red channel were considered as intracellular bacteria, while those that colocalized in both channels were considered extracellular bacteria. Correlation analysis of automated counts vs. manual counts was performed using a random subset of images ($n = 29$) from one representative experiment.

2.8. Statistical Analysis. Results are shown as mean ± SD unless stated otherwise. Statistical analyses between 2 or more categorical groups were performed using a 2-way ANOVA followed by Tukey's multiple comparisons test. Correlation analyses were done using the Pearson's correlation coefficient. A P value ≤0.05 was considered statistically significant, $*P < 0.05$, $**P < 0.01$, and $***P < 0.001$. All analyses were done using the GraphPad Prism 7.0a (GraphPad Software, San Diego).

3. Results

3.1. Development of an In Vitro Model of P. aeruginosa Long-Term Intracellular Survival in Human Airway Epithelial Cells. We sought to develop and validate a model of infection which optimized both bacterial survival and host cell viability for a period up to 120 h p.i. Airway epithelial cells (AECs) were first incubated for 4 h with *P.a.* to allow bacterial adhesion and uptake during an initial internalization phase, followed by an intracellular persistence phase where AEC were treated with tobramycin and maintained in tobramycin-containing culture medium. Tobramycin and other aminoglycosides, such as gentamicin, are cell impermeable antibiotics that kill extracellular bacteria while sparing intracellular ones and have thus been extensively used for the study of intracellular bacteria including *P.a.* [44–46, 48, 56]. In an initial experiment, we observed that the intracellular bacterial burden at 4 h p.i. was 9.5-fold higher in BEAS-2B compared to CFBE-*wt* cells grown in submerged cultures, two commonly used immortalized human epithelial cell line of bronchial origin (average of 3.5×10^4 vs. 3.7×10^3 CFU/well for BEAS-2B and CFBE-*wt*, respectively, Figure S1A-B), suggesting greater bacterial internalization in BEAS-2B cells. We thus chose to use BEAS-2B cells [57] for our model as this AEC cell line readily internalized *P.a.*

We then characterized the intracellular infection kinetics using different bacterial inoculum corresponding to a multiplicity of infection (MOI) of 0.1, 1, and 10 by assessing the intracellular bacterial burden by viable colony forming unit (CFU) count after AEC lysis and cytotoxicity by measurement of lactate dehydrogenase (LDH) release into the media. We observed that bacterial internalization (CFU count at $T = 4$ h) was relatively proportional to the MOI, with a 7-fold increase in internalization from MOI 0.1 to 1 and a 5-fold increase from MOI 1 to 10 (Figure 1(a)). After initial entry in BEAS-2B, the viable intracellular bacterial burden declined over time, with infections at MOI 10 resulting in the most rapid decline over 48 h from 1.9×10^5 CFU/well to 3.3×10^2 CFU/well, which led to near eradication of intracellular *P.a.* by 120 h p.i. In contrast, infections with MOI 1 and 0.1 resulted in only a modest decline in viable intracellular bacterial burden and allowed for significant bacterial persistence at 120 h p.i (Figure 1(a) and S1C). Notably, concomitant measurements of LDH release revealed that the marked reduction in intracellular CFU counts in cells infected at MOI 10 was associated with very high cytotoxicity (98% at 24 h to 94% at 120 h p.i) compared to MOI 1 (25.3% at 24 h and 17.4% at 120 h p.i) and 0.1 (4.9% at 24 h and 11.2% at 120 h p.i) (Figure 1(b) and Figure S1D). These results thus indicate that infection at low MOIs of 1 and 0.1 allow for long-term intracellular persistence of *P.a.* within AEC, whereas infection at MOI 10 results in a rapid

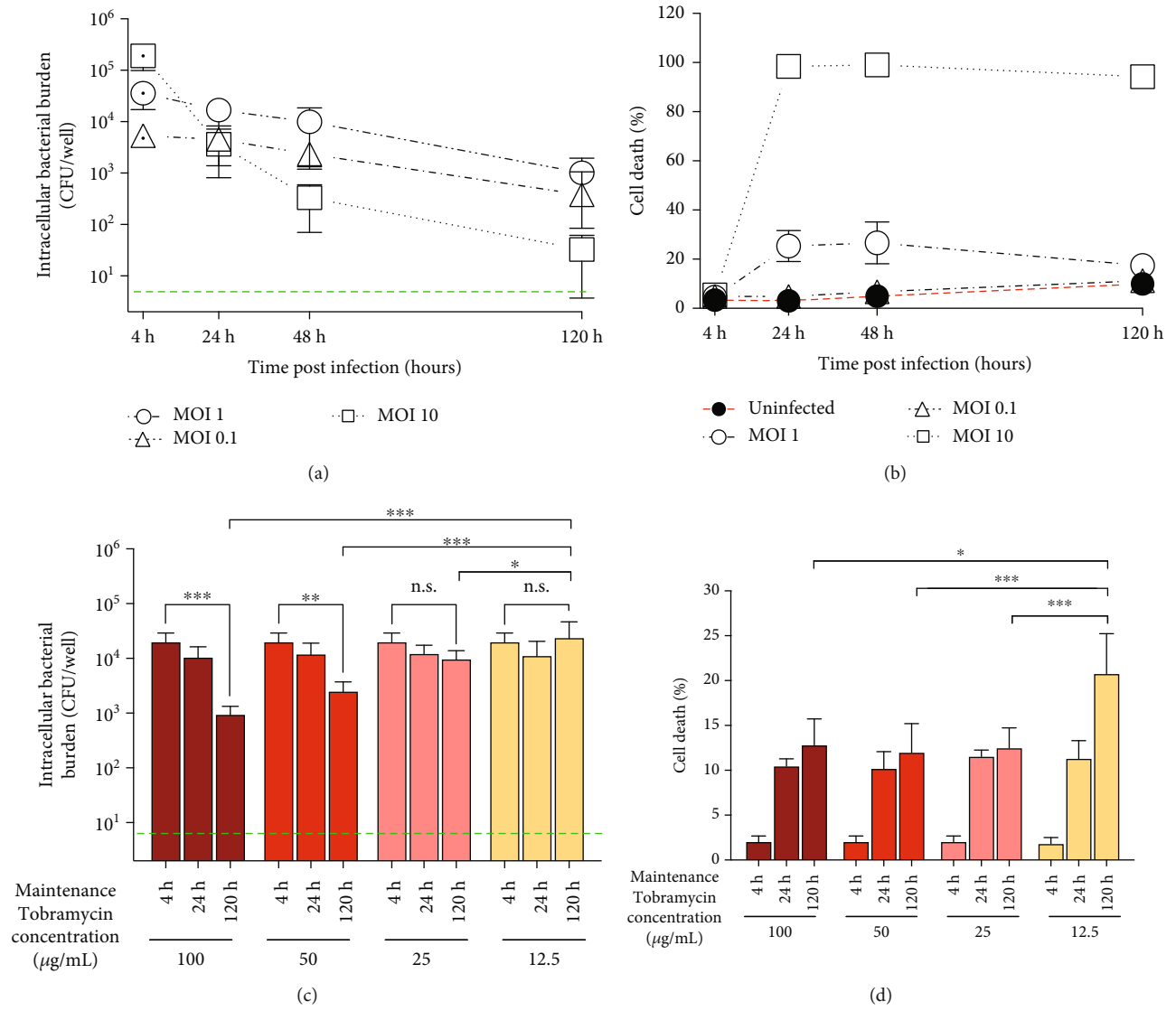

FIGURE 1: Intracellular *P.a.* survival in an airway epithelial cell infection model. (a) Intracellular bacterial burden and (b) cytotoxicity after infection with different MOI. (c) Intracellular bacterial burden and (d) cytotoxicity at different maintenance concentrations of tobramycin. For all experiments, BEAS-2B cells were infected with *P.a.* strain PAO1 at MOI 1, unless stated otherwise. After 4 h p.i., extracellular bacteria were first killed with 100 μg/mL tobramycin × 15 min for all experiments. For (a) and (b), AEC cultures were then maintained in 100 μg/mL tobramycin for the remainder of the experiment, while the tobramycin maintenance concentrations ranged from 12.5 to 100 μg/mL for (c) and (d) as indicated. The intracellular bacterial burden was measured by viable CFU count (detection limit shown as green dashed line), and cytotoxicity was measured by LDH release assay. Results shown are from data pooled from ≥4 biological replicates (≥2 independent experiments). $*P < 0.05$; $**P < 0.01$; $***P < 0.001$.

decline in intracellular bacterial counts likely attributable to extensive host cell death. We noted that the modest reduction in cell death estimates between 48 h and 120 h in AEC infected at MOI 10 (from 99.0% to 94.3%) and MOI 1 (from 26.6% to 17.4%) were likely attributable to AEC proliferation during the course of the experiment. Indeed, using total LDH as a quantitative estimate of AEC biomass (Figure S1F), we observed an average of 2.3-fold increase in AEC biomass over 5 days for all conditions except for AEC infected at MOI 10 where AEC biomass first declined significantly between 4 h and 24 h (Figure S1E).

Following the initial internalization phase, *P.a.*-infected AEC were briefly treated with tobramycin at a bactericidal concentration (100 μg/mL for 15 min) to eliminate the remaining extracellular bacteria. For the subsequent intracellular persistence phase, AEC were then maintained in culture medium containing tobramycin to inhibit any extracellular replication of bacteria released from AEC and thus avoid host cell reinfection or bacterial overgrowth in the cell culture medium. Although aminoglycosides cannot permeate cell membranes due to their anionic nature, they can still slowly accumulate intracellularly by fluid-phase endocytosis at high concentrations [58–60], a process which can influence survival of intracellular bacteria. We therefore compared the effect of different "maintenance" tobramycin concentrations (100, 50, 25, and 12.5 μg/mL) on the

infection kinetics. We observed that the tobramycin concentration did not affect intracellular bacterial counts at 24 h (Figure 1(c)). However, by 120 h, 100 and 50 μg/mL tobramycin were associated with 21- and 8-fold decrease in intracellular CFU count compared to 4 h, respectively, while 25 and 12.5 μg/mL tobramycin were not. Although the highest intracellular bacterial burden at 120 h p.i was observed with 12.5 μg/mL tobramycin, this low maintenance concentration of tobramycin also led to a significant increase of cell death, likely due to breakthrough growth of extracellular bacteria causing cell death (Figure 1(d) and Figure S1G). These results showed that the long-term survival of intracellular bacteria and AEC viability were optimal with PAO1 infection at a MOI 1 and maintenance of AEC with 25 μg/mL tobramycin.

3.2. Flow Cytometry Analysis to Assess Intracellular Infection at the Single-Cell Level. Measurement of intracellular bacterial burden by viable CFU counts allows assessment of bacterial survival in AEC on a population level but lacks resolution at the single-cell level. In order to measure both the percentage of infected AEC and the bacterial burden in individual AEC, we analyzed AEC infected with a fluorescently tagged mCherry-PAO1 strain by flow cytometry. After infection with mCherry-PAO1 using the model described above, AEC harvested at different time points were stained with fixable viability dye and analyzed for mCherry fluorescence. A gating strategy (shown in Figure S2A-C) was set using an isogenic nonfluorescent *P.a.* strain to allow for a false-positive rate of mCherry(+) AEC of <=0.5% (Figure 2(a)). We observed that 9.1% of live AEC harbored intracellular *P.a.* at 4 h p.i, a rate which decreased to 6.6% and 6.2% at 24 h and 120 h, p.i, respectively (Figure 2(c); data from all independent experiments are shown in Figure S2D-G)). We also found more cell death among AEC exposed to *P.a.* compared to uninfected AEC (10.6% vs. 5.9% at 4 h p.i, 19.7% vs. 4.3 at 24 h p.i, and 14.5% vs. 3.2 at 120 h p.i, respectively), with cell death peaking at 24 h p.i (Figure 2(d)). These results were consistent with the cytotoxicity assessment by LDH release assay (Figure 1(b)).

In order to confirm that mCherry(+) cells harbored live bacteria and that mCherry(-) cells did not, we sorted live AEC cells infected with mCherry-PAO1 at 24 h p.i into 3 different populations based on their mCherry fluorescence: mCherry negative, mCherry low, and mCherry high as shown in Figure S2H. Those AEC populations were sorted into sterile lysis buffer in pools of 10 or 100 cells per well for subsequent plating and CFU counts. No viable bacteria were recovered from mCherry-negative AEC lysates, compared to an average of 81 CFU/100 cells in mCherry-high populations and 12 CFU/100 cells in mCherry-low populations (Figure S2I). These results thus validated that most AEC from the mCherry-high populations likely harbored viable intracellular bacteria, while some cells from mCherry-low populations likely did not, and no cells from the mCherry-negative population did. Since the mCherry fluorescence histograms of mCherry-PAO1-infected AEC at 24 h p.i (Figure 2(b) and S2G) displayed a bimodal distribution, we also sought to confirm that intracellular bacteria did not lose fluorescence due to a loss of the mCherry expression plasmid. AEC lysates from the mCherry(+) populations were thus simultaneously plated for viable CFU counts on media without antibiotics and media containing carbenicillin for selection of the mCherry plasmid, and plate counts on both media showed good correlation ($r = 0.87$, Figure S2J), indicating that plasmid loss was not a significant concern.

3.3. Confocal Microscopy Imaging of P. aeruginosa-Infected Airway Epithelial Cells. To further validate the proportion of AEC harboring intracellular *P.a.* estimated by flow cytometry and determine the intracellular bacterial burden at the single-cell level, we assessed for *P.a.* in infected AEC by immunofluorescence and confocal microscopy, with differential staining of extracellular and intracellular *P.a*. At different time points, infected AEC were fixed, and extracellular bacteria were first stained with a polyclonal anti-*P.a.* antibody (AF647, red). AEC were then permeabilized and stained again with the same polyclonal anti-*P.a.* antibody (AF488, green), resulting in differential staining of extracellular and intracellular bacteria (total *P.a.* staining) (Figures 3(a) and 3(b) and Figure S3A). Intracellular *P.a.*was thus identified by their single green signal, while extracellular *P.a.*was double stained red/green. The validation of the extracellular staining was performed on bacteria spun down on coverslips without AEC and stained as previously described (Figure S3B). The absence of fluorescence spillover was assessed using single-stained infected AEC (Figure S3C).

We first analyzed the confocal microscopy images manually and estimated the percentage of infected AEC harboring intracellular *P.a.* to be 11.1% (±6.8%) at 4 h p.i and 10.6% (±0.6%) at 24 h p.i, decreasing to 3.8% (±3.1%) at 120 h p.i (Figure 3(c)). While these results were generally consistent with the flow cytometry results, small differences were noted between the different methods (11.1% vs. 9.1% at 4 h p.i, 10.6% vs. 6.6 at 24 h p.i, and 3.8% vs. 6.2% at 120 h p.i for confocal vs. flow cytometry, respectively). The bacterial burden per cell peaked at 24 h p.i (median number of bacteria per cell of 2 compared to 1 at 4 h) before decreasing at 120 h p.i (1 bacteria per cell) (Figure 3(d)). At 4 h p.i, 52% of infected cells harbored a single intracellular bacterium and less than 18% had more than two intracellular bacteria, consistent with the low MOI of 1. By 24 h p.i, 32.6% had 3 or more intracellular bacteria, possibly indicating intracellular bacterial proliferation within the first 24 h in some cells. We noted a small number of intracellular bacteria-like signal (less than 1.5%) in uninfected AEC, likely representing false-positive signals due to nonspecific binding of the secondary antibody (Figure S3A), as cultures of the AEC revealed no viable bacteria. We further validated the manual counts using an automated custom image analysis pipeline and found the two methods to be well correlated ($r = 0.906$, Figure S3D).

3.4. P. aeruginosa Clinical Isolates Display Different Intracellular Infection Kinetics. Here, we sought to compare

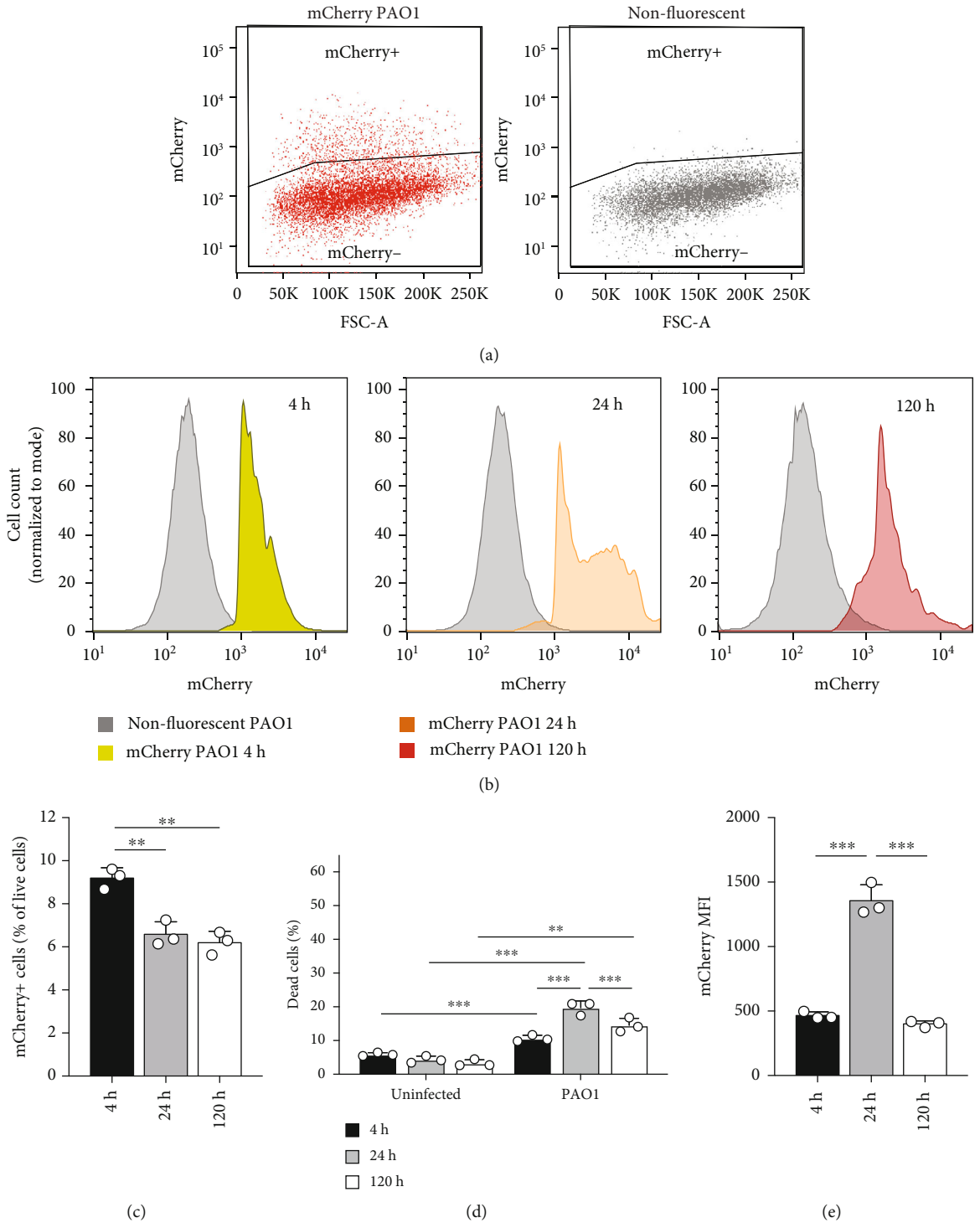

Figure 2: Analysis of *P.a.*-infected AEC by flow cytometry. (a) Gating strategy based on mCherry fluorescence intensity and forward scatter area (FSC-A) to detect mCherry(+)-infected AEC, with exclusion of mCherry(-) noninfected AEC using control samples infected with nonfluorescent PAO1. (b) mCherry fluorescence histograms of the AEC populations at different time points after infection with nonfluorescent PAO1 (whole population, grey) or mCherry PAO1 (mCherry(+) population only, colored) as indicated. Quantification of the proportion of (c) mCherry(+) AEC among all live AEC or (d) dead (FVD+) AEC among all AEC. (e) mCherry median fluorescence intensity (MFI) of the mCherry(+) AEC population at different time points after infection. The mCherry MFI of cells infected with nonfluorescent PAO1 was subtracted from the MFI of mCherry(+) cells to account for day-to-day variability in fluorescence. For all experiments, BEAS-2B cells were infected at MOI 1, except for uninfected (UI) controls. ≥20,000 cells were analyzed in each sample. For (a) and (b), representative scatter plots and histograms are shown. For (c), (d), and (e), results shown are from biological triplicates from one representative experiment of 3 independent ones (data from all 3 independent experiments are shown in Figure S2). $*P < 0.05$; $**P < 0.01$; $***P < 0.001$.

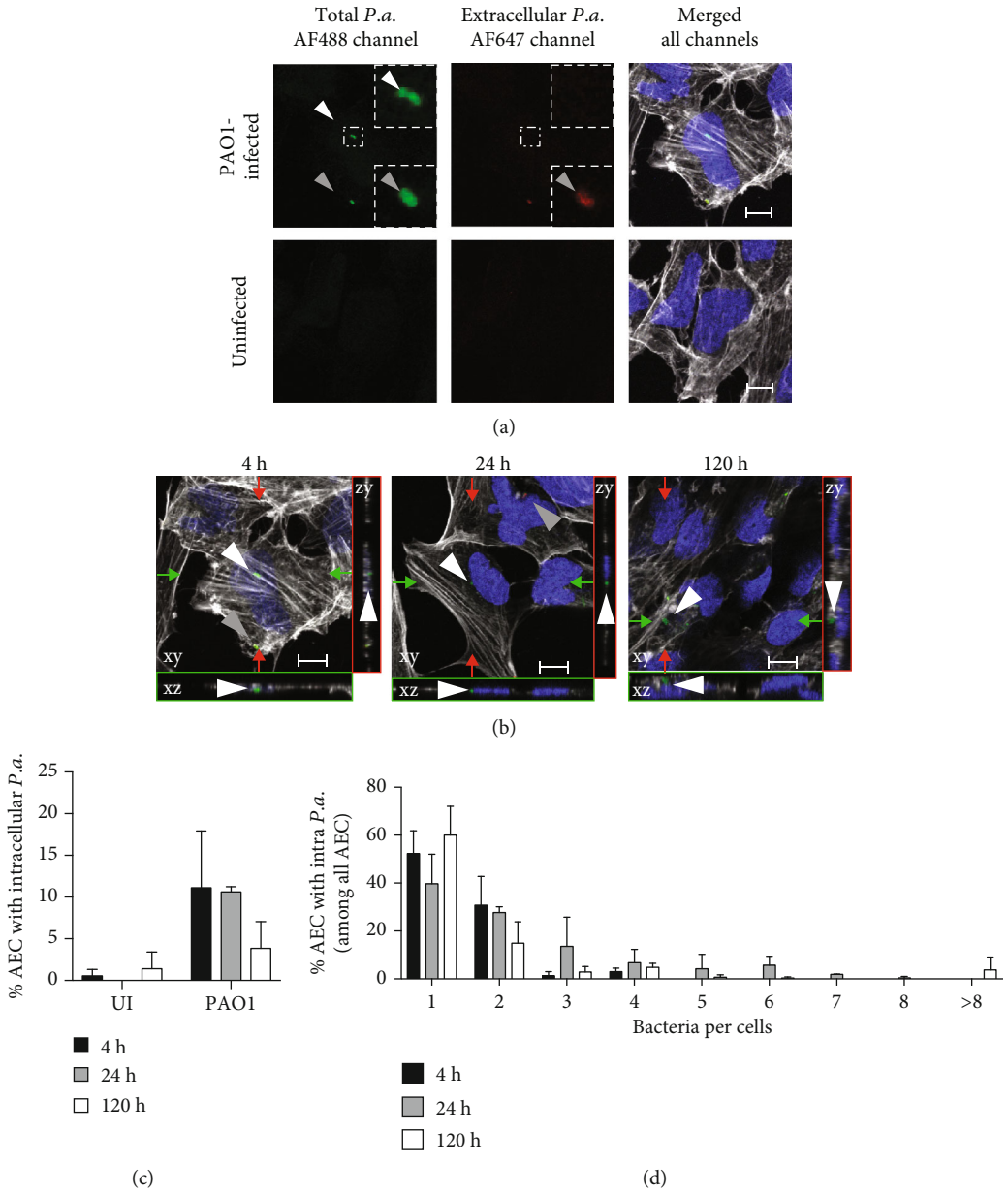

FIGURE 3: Detection of intracellular *P.a.* by confocal microscopy. (a) Z-projection images (AF488, AF647, and merged channels) to distinguish extracellular from intracellular bacteria in AEC at 4 h p.i or uninfected negative controls. (b) Z-projection and orthogonal views (merged channels) to localize bacteria at different time points. Green and red arrows denote the plane of cut for the and plane projections, respectively. Extracellular P.a. (gray arrowhead) was double-stained by the total (AF488 green) and extracellular (AF647 red) stains, while intracellular *P.a.* (white arrowhead) was single stained with the total (green) stain. The actin cytoskeleton was stained with phalloidin (grey) and the AEC nuclei with DAPI (blue). (c) The percentage of AEC harboring intracellular *P.a.* signals among all AEC. (d) The percentage of AEC harboring a given number of intracellular P.a. per AEC at different time points (among all AEC with intracellular P.a.). For all experiments, BEAS-2B cells were infected with PAO1 at MOI 1, and confocal microscopy images were analyzed manually. For (a) and (b), representative images are shown, with scale bar = 2 μm. Results in (c) and (d) shown are from pooled data ($\geq$ 1000 cells or $\geq$ 16 fields of view per conditions) from 2 independent experiments.

the long-term intracellular survival and cytotoxicity of *P.a.* clinical isolates collected from CF children (listed in supplemental Table S1-S2, [61]). The four clinical isolates displayed a range of bacterial phenotypes (e.g., mucoidy, protease and pyocyanin production, flagellar, and pilus-mediated motility (Table S2)). All were susceptible to tobramycin, and none displayed any growth defects in LB or DMEM medium (S4D-E). The bacterial burden at 4 h p.i was relatively similar in the four clinical isolates (range 1.2 to 4.2×10^4 CFU/well in BEAS-2B and 0.7 to 3.7×10^3 in CFBE-*wt*, Figure S1A), suggesting comparable internalization rates. However, we observed different

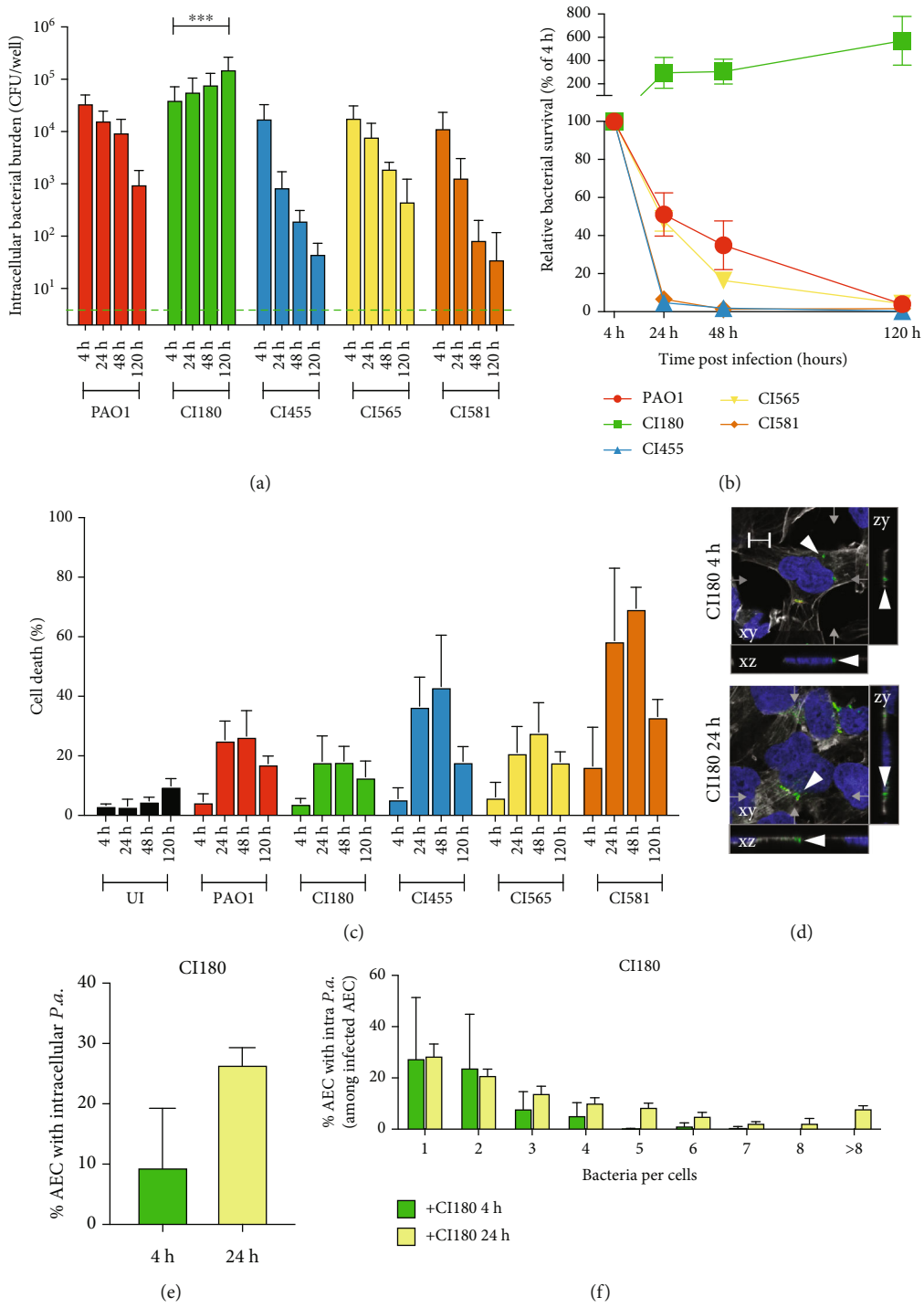

FIGURE 4: Intracellular infection kinetics and cytotoxicity of CF clinical isolates. (a) Intracellular bacterial burden, (b) relative bacterial survival, and (c) cytotoxicity over time following infection with PAO1 or clinical isolates CI180, CI455, CI565, or CI581. (d) Detection and 3D localization of intracellular *P.a.* (white arrowhead) by confocal microscopy, with evidence of clustered intracellular bacteria in AEC infected with CI180 at 24 h p.i. In AEC infected with CI180, (e) the percentage of AEC harboring intracellular *P.a.* signals among all AEC and (f) the percentage of AEC harboring a given number of bacteria per AEC at different time points (among all AEC with intracellular *P.a.*). For all experiments, BEAS-2B cells were infected with at MOI 1, except for uninfected (UI) controls. The intracellular bacterial burden was measured by viable CFU count (detection limit shown as green dashed line), and the relative bacterial survival was calculated as the intracellular bacterial burden at the indicate time normalized to the 4 h counts. The cytotoxicity was measured by LDH release assay. Confocal microscopy images were analyzed manually. Results in (a), (b), and (c) are from pooled data (≥ 6 biological replicates) from ≥3 independent experiments. Results in (b) are depicted as mean ± SEM. For (d), images representative of 3 independent experiments are shown, with scale bar = 2 μm. For (e) and (f), results are from pooled data (≥ 8 fields of view per condition) from 3 independent experiments. $*P < 0.05$; $**P < 0.01$; $***P < 0.001$.

infection kinetics over time (Figures 4(a) and 4(b) and Figure S4A). The lab strain PAO1 and 2 out of 4 clinical isolates (CI455 and CI565) persisted until 120 h p.i. (an average of 47 to 474 CFU per well were recovered at 120 h p.i.) but showed a gradual decline in intracellular bacterial burden over time. The isolate CI581 displayed the most rapid decline in intracellular bacterial burden with no detectable viable bacteria in most replicates at 120 h p.i. In contrast, the isolate CI180 displayed on average a 5.7-fold increase in intracellular bacterial counts over time, from 4.2×10^4 CFU/well at 4 h p.i and 6.0×10^4 CFU/well at 24 h p.i to 1.6×10^5 CFU/well at 120 h p.i, suggesting probable replication of intracellular bacteria given that cell death remained constant between 24 h and 120 h p.i.. We also observed that the different clinical isolates induced variable degrees of cytotoxicity over time (Figure 4(c) and Figure S4B-C). The CI180 and CI565 induced relatively limited cytotoxicity to a degree comparable to the lab strain PAO1. Conversely, CI581, which was associated with the lowest intracellular bacterial counts at 120 h p.i, caused the greatest cytotoxicity at 24 h, 48 h, and 120 h p.i. (which impaired further merasurement by confocal imaging of this strain, Figure S3E-F). Our results thus reveal that different *P.a.* isolates have divergent infection outcomes in AEC across a spectrum, from high cytotoxicity/low intracellular persistence (e.g., CI581) to low cytotoxicity/high persistence (e.g., CI180). Given the high persistence phenotype of CI180, we examined AEC infected with this clinical isolate by confocal imaging, with differential staining of *P.a.* as done with PAO1 (Figure 4(d)). We observed an increase in the proportion of AEC harboring intracellular bacteria, from 11% at 4 h p.i. to 25% at 24 h p.i. (Figure 4(e)), as well as an increase of the number of intracellular bacteria per AEC (median of 2 at 4 h p.i. vs. 3 at 24 h p.i.). Notably, at 24 h p.i, 27% AEC harbored 5 or more bacteria, including 8% AEC having 8 or more bacteria, compared to 2% with >=5 bacteria and none with >=8 bacteria at 4 h (Figure 4(f)), thus further supporting the notion that CI180 can replicate within AEC in our model.

4. Discussion

Although *P.a.* is widely known as an extracellular pathogen, many studies have demonstrated its ability to invade and survive in different models of epithelia, such as the cornea [48, 53, 62], skin [63], respiratory [31, 44], and urinary tract [50]. Bacterial survival within epithelial cells could serve as a mechanism of evasion from the immune system, extracellular host defenses, or antibiotic therapies and thus contribute to the persistent and chronic nature of *P.a.* infections. Given that most studies to date have focused on the invasion process and short-term survival of *P.a.* within epithelial cells, our understanding of the intracellular survival kinetics during long-term infection remains limited. In this study, we described an *in vitro* model of *P.a.* infection in human airway epithelial cells. Using the BEAS-2B cell line in a tobramycin protection assay, we optimized the model for intracellular bacterial persistence and demonstrated bacterial survival for up to 5 days p.i. Flow cytometry and confocal microscopy analyses allowed us to study the infection kinetics at the single-cell level, demonstrating that at low MOI, a small but reproducible proportion of AEC (~10% at 4 h p.i) internalize *P.a.*, and intracellular *P.a.* can persist for up to 5 days p.i, without causing significant host cell death. Finally, infection with different *P.a.* strains revealed that CF clinical isolates were highly heterogeneous in their ability to survive intracellularly, with CI180 providing an example of a strain with a high intracellular persistence phenotype.

P.a. has been shown to invade several epithelial cell types including the polarized kidney MDCK cells [30], corneal cells [62], and intestinal Caco-2 cells [64], as well as respiratory cells such as A549 [46, 65] and polarized AEC [47, 51]. For our study, we selected BEAS-2B cells, an AEC line widely used to study host cell signaling and inflammatory responses to *P.a.* and its secreted or surface molecules [66–69]. Previous studies using live cell video microscopy by the Fleiszig group have observed that *P.a.* can survive and replicate within epithelial cells in nonapoptotic membrane blebs [42, 43, 45, 47]. The formation of blebs is dependent on a functional T3SS and the adenylate cyclase activity of the effector proteins ExoY [45] or the ADP-ribosyltransferase activity of ExoS [42, 48], while intravesicular bacterial survival requires ExoS to avoid vesicle acidification [45, 56] or to inhibit autophagy [46]. In our model, we have not observed bleb-like structures by confocal microscopy, possibly due the specific cell line or lower MOI (1 rather than 10 or 100) used in our study or the fixation method which can collapse such structures [47].

We recognize that our current model with submerged BEAS-2B cells presents some limitations. This immortalized cell line may differ from polarized primary airway epithelial cells through display of mesenchymal-like properties [70] and thus mimic a nonpolarized or damaged epithelium [71]. Those properties are known to favor bacterial engulfment through an increased display of molecular patterns associated with bacterial invasion [31, 72, 73]. We indeed observed that bacterial internalization was 4 to 27-fold increased in BEAS-2B when compared to CFBE-*wt* cells, another commonly used bronchial epithelial cell line previously used to study AEC-*P.a.* interactions and internalization [51, 52]. The use of BEAS-2B cells thus facilitates the study of intracellular *P.a.* over time and at the single-cell level, as these are relatively rare events. Our model will therefore benefit from further validation using AEC grown at the air liquid interface, since polarization and the formation of tight junctions may influence bacterial invasion, cytotoxicity, and other host cell responses [30, 31, 69, 74].

Our model was developed to study the long-term fate of intracellular bacteria under conditions that did not cause extensive host cell death with the lab strain PAO1. The MOI of 1 results in a low frequency of AEC harboring intracellular bacteria but achieves long-term infection (up to 5 days). In contrast, the use of high MOI (such as MOI 10) results in higher rates of bacterial internalization but causes significant cytotoxicity by 24 h p.i and thus precludes any study of the long-term fate of intracellular bacteria. Gentamicin protection assays have been widely used to study intracellular *P.a.* at drug concentrations ranging from 50 to 200 μg/mL [44, 62, 75]. We

chose to use tobramycin, a chemically related aminoglycoside, for its clinical relevance in the treatment of CF lung infection [76]. While aminoglycosides (such as gentamicin and tobramycin) are impermeable to eukaryotic cells, they are slowly taken up by endocytosis over time [59], and high concentrations can impact intracellular bacterial survival and growth [58, 60]. We thus observed that reducing the maintenance concentration of tobramycin to 25 μg/mL enhanced the long-term survival of intracellular PAO1. However, the maintenance concentration was kept at 100 μg/mL during infection with CF clinical isolates to avoid growth of extracellular bacterial in *P.a.*, strains which may have varying tobramycin susceptibility.

Studies focused on long-term survival (beyond 24 h p.i) of *P.a.* in epithelial cells are scarce and have typically only assessed the intracellular bacterial burden by CFU counts [44, 51, 52, 62, 75]. Our flow cytometry and confocal microscopy analyses provided complementary approaches to estimate the percentage of infected host cells and intracellular bacterial burden at the single-cell level. Flow cytometry allowed us to analyze a large number of AEC (~50,000 cells) and was likely more selective for detection of live (metabolically active) bacteria which express mCherry fluorescence, but this method lacked the resolution to assess the number of intracellular bacteria per cell. We also recognize that flow cytometry cannot distinguish cell surface-associated bacteria from intracellular bacteria, and that a very small proportion of mCherry(+) AEC may be false-positive since our gating for mCherry(+) cells was set by our negative control to tolerate up to 0.5% false-positive fluorescence signal. Conversely, confocal microscopy was low throughput, and antibody staining of intracellular *P.a.* could not distinguish live from dead bacteria, but it provided high-resolution images that permitted confident 3D localization and counting of intracellular bacteria. We did note small differences (2 to 4%) in the proportion of *P.a.*-infected AEC estimated by confocal microscopy compared to flow cytometry, which were likely due to the different methods for bacterial detection (mCherry expression vs. antibody labeling). However, results from both methods were consistent in estimating that ~10% of AEC harbor intracellular PAO1 at 4 h p.i, with comparable trends indicating a decrease in the proportion of PAO1-infected AEC at 24 h and 120 h p.i. While it remains to be determined whether this decline was due to bacterial clearance by the host or host cell death induced by intracellular *P.a.*, we also noted that AEC proliferation during the experiment contributed to the declining estimates of the proportion of *P.a.*-infected AEC.

We then compared the intracellular survival kinetics and cytotoxicity of different *P.a.* clinical isolates from CF airway infections. While their initial intracellular bacterial burdens suggested relatively comparable rates of internalization, there were significant differences in long-term intracellular survival and cytotoxicity. We observed a high intracellular persistence phenotype in CI180, while the other strains did not persist, and CI581 was the most cytotoxic strain. Fleiszig et al. had previously reported an inverse correlation between cytotoxicity and intracellular invasion of MDCK kidney epithelial cells upon testing of *P.a.* isolates from corneal infections, but the study did not examine time points beyond 3 h p.i [53]. More recent studies assessed a few CF clinical isolates for intracellular bacterial survival and cytotoxicity up until 24 h p.i in immortalized airway epithelial cells and described clinical isolates with a persistent intracellular infection phenotype reminiscent of what we observed with CI180 [51, 52]. Using a model of bladder epithelial cell infection, Penaranda et al. also observed a comparable intracellular persistence in certain *P.a.* clinical isolates originating from urinary tract infections [50]. The bacterial functions that might contribute to strain-specific intracellular persistence are likely numerous but remain incompletely understood. These include mechanisms that directly enhance bacterial survival and/or replication, such as the ability to metabolically adapt to the intracellular host milieu [50, 52], or indirectly modulate host cell viability or responses, such as the expression of the T3SS, effectors proteins, and other secreted cytotoxic factors [42, 45, 48, 56, 77–79]. The ability of certain clinical isolates to successfully persist in AEC raises the possibility that these host-adapted *P.a.* strains harbor phenotypic characteristics that promote their ability to cause chronic human infections. Our model would enable future mechanistic studies to understand the host-pathogen interactions and bacterial factors involved in long-term intracellular persistence of *P.a.* in airway epithelial cells.

Data Availability

The data supporting our results are shown in the main and supplemental figures, as indicated in the manuscript. Raw images used for analysis are available at https://omero.med.ualberta.ca/webclient/?show=dataset-1152.

Disclosure

Some of this work was previously presented as part of a meeting abstract as per URL: https://www.atsjournals.org/doi/abs/10.1164/ajrccmconference.2018.197.1_MeetingAbstracts.A6262

Conflicts of Interest

The authors declare no conflicts of interest.

Authors' Contributions

Julien K. Malet, Lisa C. Hennemann, Emmanuel Faure, Simon Rousseau, and Dao Nguyen conceived the study. Julien K. Malet, Lisa C. Hennemann, and Elizabeth Hua performed the experimental work. Valerie Waters provided data and bacterial strains. Julien K. Malet, Lisa C. Hennemann, and Dao Nguyen analyzed the data. Julien K. Malet, Lisa C. Hennemann, Simon Rousseau, Valerie Waters, and Dao Nguyen wrote and revised the manuscript. Julien K. Malet and Lisa C. Hennemann contributed equally to this work.

Acknowledgments

This study was supported by research funding from the Cystic Fibrosis Canada (559985 to D.N) and the US Cystic Fibrosis Foundation (NGUYEN21I0 to D.N), salary support from the Fonds de Recherche du Quebec Santé (D.N), and scholarships from the Fonds de Recherche du Quebec Santé (to K.J.M), the Reseau en Santé Respiratoire (to K.J.M and L.H), and the Deutscher Akademischer Austauschdienst (to L.H). We thank the Immunophenotyping Platform at the Research Institute of the McGill University Health Centre (RI-MUHC) for their assistance with the cell sorting. We thank Sam Moskowitz for providing the mCherry (pMKB1) plasmid.

Supplementary Materials

Supplemental Figure S1–S4, Table S1-S2 and Methods. *(Supplementary Materials)*

References

[1] G. G. Anderson, K. W. Dodson, T. M. Hooton, and S. J. Hultgren, "Intracellular bacterial communities of uropathogenic in urinary tract pathogenesis," *Trends in Microbiology*, vol. 12, no. 9, pp. 424–430, 2004.

[2] F. Peyrusson, H. Varet, T. K. Nguyen et al., "Intracellular Staphylococcus aureus persisters upon antibiotic exposure," *Nature Communications*, vol. 11, no. 1, p. 2200, 2020.

[3] D. A. Hunstad and S. S. Justice, "Intracellular lifestyles and immune evasion strategies of uropathogenic Escherichia coli," *Annual Review of Microbiology*, vol. 64, no. 1, pp. 203–221, 2010.

[4] I. U. Mysorekar and S. J. Hultgren, "Mechanisms of uropathogenic Escherichia coli persistence and eradication from the urinary tract," *Proceedings of the National Academy of Sciences*, vol. 103, no. 38, pp. 14170–14175, 2006.

[5] C. Martínez-Figueroa, K. Cortés-Sarabia, L. del Carmen Alarcón-Romero, H. G. Catalán-Nájera, M. Martínez-Alarcón, and A. Vences-Velázquez, "Observation of intracellular bacterial communities in urinary sediment using brightfield microscopy; a case report," *BMC Urology*, vol. 20, no. 1, p. 89, 2020.

[6] D. A. Rosen, T. M. Hooton, W. E. Stamm, P. A. Humphrey, and S. J. Hultgren, "Detection of intracellular bacterial communities in human urinary tract infection," *PLoS Medicine*, vol. 4, no. 12, article e329, 2007.

[7] G. Rollin, X. Tan, F. Tros et al., "Intracellular survival of Staphylococcus aureus in endothelial cells: a matter of growth or persistence," *Frontiers in Microbiology*, vol. 8, p. 1354, 2017.

[8] M. Strobel, H. Pförtner, L. Tuchscherr et al., "Post-invasion events after infection with Staphylococcus aureus are strongly dependent on both the host cell type and the infecting S. aureus strain," *Clinical Microbiology and Infection*, vol. 22, no. 9, pp. 799–809, 2016.

[9] E. G. Vozza, M. E. Mulcahy, and R. M. McLoughlin, "Making the most of the host; targeting the autophagy pathway facilitates Staphylococcus aureus intracellular survival in neutrophils," *Frontiers in Immunology*, vol. 12, p. 667387, 2021.

[10] R. A. Almeida, K. R. Matthews, E. Cifrian, A. J. Guidry, and S. P. Oliver, "Staphylococcus aureus invasion of bovine mammary epithelial cells," *Journal of Dairy Science*, vol. 79, no. 6, pp. 1021–1026, 1996.

[11] S. Clement, P. Vaudaux, P. Francois et al., "Evidence of an intracellular reservoir in the nasal mucosa of patients with recurrent Staphylococcus aureus rhinosinusitis," *The Journal of Infectious Diseases*, vol. 192, no. 6, pp. 1023–1028, 2005.

[12] J. K. Ellington, M. Harris, L. Webb et al., "Intracellular Staphylococcus aureus. A mechanism for the indolence of osteomyelitis," *The Journal of Bone and Joint Surgery. British Volume*, vol. 85, no. 6, pp. 918–921, 2003.

[13] S. S. Reilly, M. C. Hudson, J. F. Kellam, and W. K. Ramp, "In vivo internalization of Staphylococcus aureus by embryonic chick osteoblasts," *Bone*, vol. 26, no. 1, pp. 63–70, 2000.

[14] S. Duraiswamy, J. L. Y. Chee, S. Chen, E. Yang, K. Lees, and S. L. Chen, "Purification of intracellular bacterial communities during experimental urinary tract infection reveals an abundant and viable bacterial reservoir," *Infection and Immunity*, vol. 86, no. 4, p. e00740, 2018.

[15] V. C. S. Scott, D. A. Haake, B. M. Churchill, S. S. Justice, and J.-H. Kim, "Intracellular bacterial communities: a potential etiology for chronic lower urinary tract symptoms," *Urology*, vol. 86, no. 3, pp. 425–431, 2015.

[16] C. D. Morin, E. Déziel, J. Gauthier, R. C. Levesque, and G. W. Lau, "An organ system-based synopsis of Pseudomonas aeruginosa virulence," *Virulence*, vol. 12, no. 1, pp. 1469–1507, 2021.

[17] M. Shteinberg, I. J. Haq, D. Polineni, and J. C. Davies, "Cystic fibrosis," *Lancet*, vol. 397, no. 10290, pp. 2195–2211, 2021.

[18] R. S. Baltimore, C. D. Christie, and G. J. Smith, "Immunohistopathologic localization of Pseudomonas aeruginosa in lungs from patients with cystic fibrosis. Implications for the pathogenesis of progressive lung deterioration," *The American Review of Respiratory Disease*, vol. 140, no. 6, pp. 1650–1661, 1989.

[19] T. Bjarnsholt, P. Ø. Jensen, M. J. Fiandaca et al., "Pseudomonas aeruginosa biofilms in the respiratory tract of cystic fibrosis patients," *Pediatric Pulmonology*, vol. 44, no. 6, pp. 547–558, 2009.

[20] S. B. Potts, V. L. Roggli, and A. Spock, "Immunohistologic quantification of Pseudomonas aeruginosa in the tracheobronchial tree from patients with cystic fibrosis," *Pediatric Pathology & Laboratory Medicine*, vol. 15, no. 5, pp. 707–721, 1995.

[21] P. K. Singh, A. L. Schaefer, M. R. Parsek, T. O. Moninger, M. J. Welsh, and E. P. Greenberg, "Quorum-sensing signals indicate that cystic fibrosis lungs are infected with bacterial biofilms," *Nature*, vol. 407, no. 6805, pp. 762–764, 2000.

[22] O. Ciofu and T. Tolker-Nielsen, "Tolerance and resistance of Pseudomonas aeruginosa biofilms to antimicrobial agents-how P. aeruginosa can escape antibiotics," *Frontiers in Microbiology*, vol. 10, p. 913, 2019.

[23] N. M. Maurice, B. Bedi, and R. T. Sadikot, "Pseudomonas aeruginosa biofilms: host response and clinical implications in lung infections," *American Journal of Respiratory Cell and Molecular Biology*, vol. 58, no. 4, pp. 428–439, 2018.

[24] E. Faure, K. Kwong, and D. Nguyen, "Pseudomonas aeruginosa in chronic lung infections: how to adapt within the host?," *Frontiers in Immunology*, vol. 9, p. 2416, 2018.

[25] Y. Sun, M. Karmakar, P. R. Taylor, A. Rietsch, and E. Pearlman, "ExoS and ExoT ADP ribosyltransferase activities mediate Pseudomonas aeruginosa keratitis by promoting

neutrophil apoptosis and bacterial survival," *Journal of Immunology (Baltimore, Md. : 1950)*, vol. 188, no. 4, pp. 1884–1895, 2012.

[26] F. Bastaert, S. Kheir, V. Saint-Criq et al., "Pseudomonas aeruginosa LasB subverts alveolar macrophage activity by interfering with bacterial killing through downregulation of innate immune defense, reactive oxygen species generation, and complement activation," *Frontiers in Immunology*, vol. 9, p. 1675, 2018.

[27] K. G. Leidal, K. L. Munson, M. C. Johnson, and G. M. Denning, "Metalloproteases from Pseudomonas aeruginosa degrade human RANTES, MCP-1, and ENA-78," *Journal of Interferon & Cytokine Research*, vol. 23, no. 6, pp. 307–318, 2003.

[28] V. Saint-Criq, B. Villeret, F. Bastaert et al., "Pseudomonas aeruginosaLasB protease impairs innate immunity in mice and humans by targeting a lung epithelial cystic fibrosis transmembrane regulator–IL-6–antimicrobial–repair pathway," *Thorax*, vol. 73, no. 1, pp. 49–61, 2018.

[29] J. S. Gunn, L. O. Bakaletz, and D. J. Wozniak, "What's on the outside matters: the role of the extracellular polymeric substance of gram-negative biofilms in evading host immunity and as a target for therapeutic intervention," *The Journal of Biological Chemistry*, vol. 291, no. 24, pp. 12538–12546, 2016.

[30] I. Bucior, K. Mostov, and J. N. Engel, "Pseudomonas aeruginosa-mediated damage requires distinct receptors at the apical and basolateral surfaces of the polarized epithelium," *Infection and Immunity*, vol. 78, no. 3, pp. 939–953, 2010.

[31] I. Bucior, J. F. Pielage, and J. N. Engel, "Pseudomonas aeruginosa pili and flagella mediate distinct binding and signaling events at the apical and basolateral surface of airway epithelium," *PLoS Pathogens*, vol. 8, no. 4, article e1002616, 2012.

[32] T. Eierhoff, B. Bastian, R. Thuenauer et al., "A lipid zipper triggers bacterial invasion," *Proceedings of the National Academy of Sciences*, vol. 111, no. 35, pp. 12895–12900, 2014.

[33] R. W. Heiniger, H. C. Winther-Larsen, R. J. Pickles, M. Koomey, and M. C. Wolfgang, "Infection of human mucosal tissue by Pseudomonas aeruginosa requires sequential and mutually dependent virulence factors and a novel pilus-associated adhesin," *Cellular Microbiology*, vol. 12, no. 8, pp. 1158–1173, 2010.

[34] A. O. Azghani, S. Idell, M. Bains, and R. E. W. Hancock, "Pseudomonas aeruginosa outer membrane protein F is an adhesin in bacterial binding to lung epithelial cells in culture," *Microbial Pathogenesis*, vol. 33, no. 3, pp. 109–114, 2002.

[35] T. S. Zaidi, S. M. Fleiszig, M. J. Preston, J. B. Goldberg, and G. B. Pier, "Lipopolysaccharide outer core is a ligand for corneal cell binding and ingestion of Pseudomonas aeruginosa," *Investigative Ophthalmology & Visual Science*, vol. 37, no. 6, pp. 976–986, 1996.

[36] B. I. Kazmierczak, T. S. Jou, K. Mostov, and J. N. Engel, "Rho GTPase activity modulates Pseudomonas aeruginosa internalization by epithelial cells," *Cellular Microbiology*, vol. 3, no. 2, pp. 85–98, 2001.

[37] J. F. Pielage, K. R. Powell, D. Kalman, and J. N. Engel, "RNAi screen reveals an Abl kinase-dependent host cell pathway involved in Pseudomonas aeruginosa internalization," *PLoS Pathogens*, vol. 4, no. 3, article e1000031, 2008.

[38] A. Kierbel, A. Gassama-Diagne, K. Mostov, and J. N. Engel, "The phosphoinositol-3-kinase-protein kinase B/Akt pathway is critical for Pseudomonas aeruginosa strain PAK internalization," *Molecular Biology of the Cell*, vol. 16, no. 5, pp. 2577–2585, 2005.

[39] P. Lepanto, D. M. Bryant, J. Rossello, A. Datta, K. E. Mostov, and A. Kierbel, "Pseudomonas aeruginosa interacts with epithelial cells rapidly forming aggregates that are internalized by a Lyn-dependent mechanism," *Cellular Microbiology*, vol. 13, no. 8, pp. 1212–1222, 2011.

[40] M. Esen, H. Grassmé, J. Riethmüller, A. Riehle, K. Fassbender, and E. Gulbins, "Invasion of human epithelial cells by Pseudomonas aeruginosa involves Src-like tyrosine kinases p60Src and p59Fyn," *Infection and Immunity*, vol. 69, no. 1, pp. 281–287, 2001.

[41] D. J. Evans, T. C. Kuo, M. Kwong, R. Van, and S. M. J. Fleiszig, "Mutation of csk, encoding the C-terminal Src kinase, reduces Pseudomonas aeruginosa internalization by mammalian cells and enhances bacterial cytotoxicity," *Microbial Pathogenesis*, vol. 33, no. 3, pp. 135–143, 2002.

[42] A. A. Angus, D. J. Evans, J. T. Barbieri, and S. M. J. Fleiszig, "The ADP-ribosylation domain of Pseudomonas aeruginosa ExoS is required for membrane bleb niche formation and bacterial survival within epithelial cells," *Infection and Immunity*, vol. 78, no. 11, pp. 4500–4510, 2010.

[43] A. A. Angus, A. A. Lee, D. K. Augustin, E. J. Lee, D. J. Evans, and S. M. J. Fleiszig, "Pseudomonas aeruginosa induces membrane blebs in epithelial cells, which are utilized as a niche for intracellular replication and motility," *Infection and Immunity*, vol. 76, no. 5, pp. 1992–2001, 2008.

[44] R. Garcia-Medina, W. M. Dunne, P. K. Singh, and S. L. Brody, "Pseudomonas aeruginosa acquires biofilm-like properties within airway epithelial cells," *Infection and Immunity*, vol. 73, no. 12, pp. 8298–8305, 2005.

[45] V. Hritonenko, J. J. Mun, C. Tam et al., "Adenylate cyclase activity of Pseudomonas aeruginosa ExoY can mediate bleb-niche formation in epithelial cells and contributes to virulence," *Microbial Pathogenesis*, vol. 51, no. 5, pp. 305–312, 2011.

[46] L. Rao, I. De La Rosa, Y. Xu et al., "Pseudomonas aeruginosa survives in epithelia by ExoS-mediated inhibition of autophagy and mTOR," *EMBO Reports*, vol. 22, no. 2, article e50613, 2021.

[47] A. L. Jolly, D. Takawira, O. O. Oke et al., "Pseudomonas aeruginosa-induced bleb-niche formation in epithelial cells is independent of actinomyosin contraction and enhanced by loss of cystic fibrosis transmembrane-conductance regulator osmoregulatory function," *MBio*, vol. 6, no. 2, article e02533, 2015.

[48] A. R. Kroken, C. K. Chen, D. J. Evans, T. L. Yahr, and S. M. J. Fleiszig, "The impact of ExoS on Pseudomonas aeruginosa internalization by epithelial cells is independent of fleQ and correlates with bistability of type three secretion system gene expression," *MBio*, vol. 9, no. 3, p. e00668, 2018.

[49] G. G. Anderson, J. J. Palermo, J. D. Schilling, R. Roth, J. Heuser, and S. J. Hultgren, "Intracellular bacterial biofilm-like pods in urinary tract infections," *Science*, vol. 301, no. 5629, pp. 105–107, 2003.

[50] C. Penaranda, N. M. Chumbler, and D. T. Hung, "Dual transcriptional analysis reveals adaptation of host and pathogen to intracellular survival of Pseudomonas aeruginosa associated with urinary tract infection," *PLoS Pathogens*, vol. 17, no. 4, article e1009534, 2021.

[51] K. E. A. Darling, A. Dewar, and T. J. Evans, "Role of the cystic fibrosis transmembrane conductance regulator in

internalization of Pseudomonas aeruginosa by polarized respiratory epithelial cells," *Cellular Microbiology*, vol. 6, no. 6, pp. 521–533, 2004.

[52] M. Del Mar Cendra and E. Torrents, "Differential adaptability between reference strains and clinical isolates of Pseudomonas aeruginosa into the lung epithelium intracellular lifestyle," *Virulence*, vol. 11, no. 1, pp. 862–876, 2020.

[53] S. M. Fleiszig, T. S. Zaidi, M. J. Preston, M. Grout, D. J. Evans, and G. B. Pier, "Relationship between cytotoxicity and corneal epithelial cell invasion by clinical isolates of Pseudomonas aeruginosa," *Infection and Immunity*, vol. 64, no. 6, pp. 2288–2294, 1996.

[54] J. Schindelin, I. Arganda-Carreras, E. Frise et al., "Fiji: an open-source platform for biological-image analysis," *Nature Methods*, vol. 9, no. 7, pp. 676–682, 2012.

[55] F. de Chaumont, S. Dallongeville, N. Chenouard et al., "Icy: an open bioimage informatics platform for extended reproducible research," *Nature Methods*, vol. 9, no. 7, pp. 690–696, 2012.

[56] S. R. Heimer, D. J. Evans, M. E. Stern, J. T. Barbieri, T. Yahr, and S. M. J. Fleiszig, "Pseudomonas aeruginosa utilizes the type III secreted toxin ExoS to avoid acidified compartments within epithelial cells," *PLoS One*, vol. 8, no. 9, article e73111, 2013.

[57] R. R. Reddel, Y. Ke, B. I. Gerwin et al., "Transformation of human bronchial epithelial cells by infection with SV40 or adenovirus-12 SV40 hybrid virus, or transfection via strontium phosphate coprecipitation with a plasmid containing SV40 early region genes," *Cancer Research*, vol. 48, no. 7, pp. 1904–1909, 1988.

[58] M. Kortebi, E. Milohanic, G. Mitchell et al., "Listeria monocytogenes switches from dissemination to persistence by adopting a vacuolar lifestyle in epithelial cells," *PLoS Pathogens*, vol. 13, no. 11, article e1006734, 2017.

[59] M. Takano, Y. Ohishi, M. Okuda, M. Yasuhara, and R. Hori, "Transport of gentamicin and fluid-phase endocytosis markers in the LLC-PK1 kidney epithelial cell line," *The Journal of Pharmacology and Experimental Therapeutics*, vol. 268, no. 2, pp. 669–674, 1994.

[60] T. T. VanCleave, A. R. Pulsifer, M. G. Connor, J. M. Warawa, and M. B. Lawrenz, "Impact of gentamicin concentration and exposure time on intracellular Yersinia pestis," *Frontiers in Cellular and Infection Microbiology*, vol. 7, p. 505, 2017.

[61] P. Vidya, L. Smith, T. Beaudoin et al., "Chronic infection phenotypes of Pseudomonas aeruginosa are associated with failure of eradication in children with cystic fibrosis," *European Journal of Clinical Microbiology & Infectious Diseases*, vol. 35, no. 1, pp. 67–74, 2016.

[62] S. M. Fleiszig, T. S. Zaidi, and G. B. Pier, "Pseudomonas aeruginosa invasion of and multiplication within corneal epithelial cells in vitro," *Infection and Immunity*, vol. 63, no. 10, pp. 4072–4077, 1995.

[63] P. M. Alves, E. Al-Badi, C. Withycombe, P. M. Jones, K. J. Purdy, and S. E. Maddocks, "Interaction between Staphylococcus aureus and Pseudomonas aeruginosa is beneficial for colonisation and pathogenicity in a mixed biofilm," *Pathogens and Disease*, vol. 76, no. 1, 2018.

[64] S. H. M. Pereira, M. P. Cervante, S. Bentzmannde, and M. C. Plotkowski, "Pseudomonas aeruginosa entry into Caco-2 cells is enhanced in repairing wounded monolayers," *Microbial Pathogenesis*, vol. 23, no. 4, pp. 249–255, 1997.

[65] E. Chi, T. Mehl, D. Nunn, and S. Lory, "Interaction of Pseudomonas aeruginosa with A549 pneumocyte cells," *Infection and Immunity*, vol. 59, no. 3, pp. 822–828, 1991.

[66] L. C. Hennemann, S. L. LaFayette, J. K. Malet et al., "LasR-deficient Pseudomonas aeruginosa variants increase airway epithelial mICAM-1 expression and enhance neutrophilic lung inflammation," *PLoS Pathogens*, vol. 17, no. 3, article e1009375, 2021.

[67] S. L. LaFayette, D. Houle, T. Beaudoin et al., "Cystic fibrosis–adapted Pseudomonas aeruginosa quorum sensing lasR mutants cause hyperinflammatory responses," *Science Advances*, vol. 1, no. 6, article e1500199, 2015.

[68] W. Liu, T. Sun, and Y. Wang, "Integrin $\alpha v\beta 6$ mediates epithelial-mesenchymal transition in human bronchial epithelial cells induced by lipopolysaccharides of Pseudomonas aeruginosa via TGF-β1-Smad2/3 signaling pathway," *Folia Microbiologica*, vol. 65, no. 2, pp. 329–338, 2020.

[69] M.-C. Plotkowski, B. A. Brandão, M.-C. de Assis et al., "Lipid body mobilization in the ExoU-induced release of inflammatory mediators by airway epithelial cells," *Microbial Pathogenesis*, vol. 45, no. 1, pp. 30–37, 2008.

[70] X. Han, T. Na, T. Wu, and B. Z. Yuan, "Human lung epithelial BEAS-2B cells exhibit characteristics of mesenchymal stem cells," *PLoS One*, vol. 15, no. 1, article e0227174, 2020.

[71] C. E. Stewart, E. E. Torr, N. H. Mohd Jamili, C. Bosquillon, and I. Sayers, "Evaluation of differentiated human bronchial epithelial cell culture systems for asthma research," *The Journal of Allergy*, vol. 2012, article 943982, 11 pages, 2012.

[72] A. Kierbel, A. Gassama-Diagne, C. Rocha et al., "Pseudomonas aeruginosa exploits a PIP3-dependent pathway to transform apical into basolateral membrane," *The Journal of Cell Biology*, vol. 177, no. 1, pp. 21–27, 2007.

[73] M. C. Plotkowski, S. de Bentzmann, S. H. Pereira et al., "Pseudomonas aeruginosa internalization by human epithelial respiratory cells depends on cell differentiation, polarity, and junctional complex integrity," *American Journal of Respiratory Cell and Molecular Biology*, vol. 20, no. 5, pp. 880–890, 1999.

[74] B. I. Kazmierczak, K. Mostov, and J. N. Engel, "Epithelial cell polarity alters Rho-GTPase responses to Pseudomonas aeruginosa," *Molecular Biology of the Cell*, vol. 15, no. 2, pp. 411–419, 2004.

[75] U. Ha and S. Jin, "Growth phase-dependent invasion of Pseudomonas aeruginosa and its survival within HeLa cells," *Infection and Immunity*, vol. 69, no. 7, pp. 4398–4406, 2001.

[76] F. Ratjen, F. Brockhaus, and G. Angyalosi, "Aminoglycoside therapy against Pseudomonas aeruginosa in cystic fibrosis: a review," *Journal of Cystic Fibrosis*, vol. 8, no. 6, pp. 361–369, 2009.

[77] V. Finck-Barbançon, J. Goranson, L. Zhu et al., "ExoU expression byPseudomonas aeruginosa correlates with acute cytotoxicity and epithelial injury," *Molecular Microbiology*, vol. 25, no. 3, pp. 547–557, 1997.

[78] Y. Q. O'Malley, M. Y. Abdalla, M. L. McCormick, K. J. Reszka, G. M. Denning, and B. E. Britigan, "Subcellular localization of Pseudomonas pyocyanin cytotoxicity in human lung epithelial cells," *Lung Cellular and Molecular Physiology*, vol. 284, no. 2, pp. L420–L430, 2003.

[79] S. H. Shafikhani, C. Morales, and J. Engel, "The Pseudomonas aeruginosa type III secreted toxin ExoT is necessary and sufficient to induce apoptosis in epithelial cells," *Cellular Microbiology*, vol. 10, no. 4, pp. 994–1007, 2008.